



HAL
open science

Validation of the simulation software civa Ut in separated transmit/receive configurations

F. Foucher, S. Lonne, G. Toullelan, S. Mahaut, Sylvain Chatillon, E. Schumacher

► **To cite this version:**

F. Foucher, S. Lonne, G. Toullelan, S. Mahaut, Sylvain Chatillon, et al.. Validation of the simulation software civa Ut in separated transmit/receive configurations. 56th Annual Conference of the British Institute of Non-Destructive Testing, NDT 2017, 2017, Telford, United Kingdom. cea-01843011

HAL Id: cea-01843011

<https://cea.hal.science/cea-01843011v1>

Submitted on 22 Jan 2024

HAL is a multi-disciplinary open access archive for the deposit and dissemination of scientific research documents, whether they are published or not. The documents may come from teaching and research institutions in France or abroad, or from public or private research centers.

L'archive ouverte pluridisciplinaire **HAL**, est destinée au dépôt et à la diffusion de documents scientifiques de niveau recherche, publiés ou non, émanant des établissements d'enseignement et de recherche français ou étrangers, des laboratoires publics ou privés.

VALIDATION OF THE SIMULATION SOFTWARE CIVA UT IN SEPARATED TRANSMIT/RECEIVE CONFIGURATIONS

Fabrice FOUCHER¹, Sébastien LONNE¹,
Gwénaél TOULLELAN², Steve MAHAUT², Sylvain CHATILLON², Erica SCHUMACHER³

¹ EXTENDE, Le Bergson, 15 Avenue Emile Baudot, 91300 Massy, France
fabrice.foucher@extende.com

² CEA, LIST, 91191 Gif-sur-Yvette, France
gwenael.toullelan@cea.fr, steve.mahaut@cea.fr, sylvain.chatillon@cea.fr

³ EXTENDE Inc., PO Box 461, Ballston Spa, New York, USA
erica.schumacher@extende.com

Abstract

Numerical modelling is widely used in the framework of inspection qualification processes, since it offers the capability to study a wide scope of configurations and at a lower cost compared to a full experimental campaign. In this context, the reliability of simulation models is of the highest importance. In order to evaluate this reliability and determine the field of application of CIVA simulation tools, a long-range collaborative work has been engaged between the CEA-LIST & EXTENDE. This is based on comparisons between experimental results and CIVA predictions on configurations representative of industrial NDT applications. After an overview of the validation works initiated, this paper focuses on the presentation of results obtained in tandem mode, a UT technique commonly used for the detection of side wall weld defects, such as in the zonal discrimination method. In this configuration, a pair of single element transducers located one after the other scans the part, one being the transmitter and the other being the receiver. This technique can also use a phased-array probe with two separate groups of elements. The comparisons between experimental and simulated results obtained on such configurations are presented in this paper.

1. Introduction

The Ultrasounds Testing module of CIVA [1] uses ray-based beam computation models and interaction algorithms to compute the beam scattered by a defect or by the specimen boundaries. These models are mainly based on semi-analytical formulations and numeric integrals [2]. In order to evaluate their reliability, an experimental characterization procedure of these models is followed [3], which includes: Defining and performing experiments, precisely describing the relevant and corresponding input parameters in CIVA, and conducting the simulations with CIVA, and comparing the simulated results with experimental ones.

In this paper some results obtained in separate Transmit/Receive configurations widely used industrially are described, weld UT inspections for instance. For each presented case, a depiction of how to properly describe input parameters is provided. Most of the presented results are publicly available on the EXTENDE website [4]. You will also find many other experimental validation results there such as: side drilled hole and flat bottom hole (FBH) responses in various calibration blocks and for various inspection techniques (immersion, contact), corner echoes obtained with pressure waves and shear waves, TOFD configurations, phased-array UT cases, geometrical echoes studies, multi skips inspection configurations, etc. Some validation results with the Eddy Current module of CIVA are also available on the website.

2. Dual Element probe characterization

A Dual Element probe uses two crystals, one for beam transmission and one for reception, separated by an acoustic barrier. This type of transducer is quite commonly used in order to inspect strongly attenuating materials, or to detect near surface defects, thanks to the natural ability of such probes to remove the entry surface echo.

In this experimental characterization study, FBH reflectors are used. The transducer used is a 4MHz transducer on a Plexiglas wedge designed to generate a 45° longitudinal wave in stainless steel.

2.1 Description of the Dual Element probe and of the CIVA simulation configuration

For such probes, the necessary input data for the simulation is often difficult to obtain, especially because of the lack of information from the manufacturer, and also the lack of standardization of the data provided from one manufacturer to another. This applies mostly for the wedge various angles (roof and incidence angle) but also regarding the T and R crystal separation distance or the acoustic properties of the wedge itself. For all these reasons, it is sometimes necessary to do Radiographic or Computed Tomography acquisitions and analysis on such probes to find out the relevant values. On the following images, a picture of such a probe can be seen as well as its 3D view in CIVA after entering the right parameters. As some of the angles are very sensitive to the results, another very efficient approach which facilitates overcoming the uncertainties of the input data can be used. This process is based on a reverse engineering applied on the DAC curves analysis and is presented in [5].

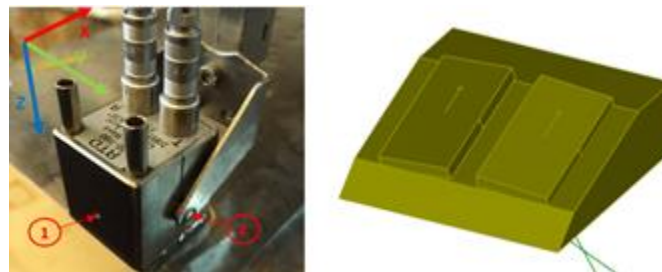


Figure 1. Dual Element Transducer and its description in CIVA.

The transducer response has been evaluated on a calibration block made of ferritic steel and where several FBHs have been inserted. To simulate FBH echoes, the KIRCHHOFF model has been used.

Two simulations have been performed:

- One computation with a plane wave approximation used for the incident beam description (mentioned as « KIR » in the following part of the paper).
- One computation with a more precise description of the acoustic beam, the « Full wave » option, now available in CIVA. Results obtained with this model will be written down as « KIR COMPLETE BEAM» in this paper.

2.2 Acquisitions performed

C-scan acquisitions have been performed and the direct signals obtained from the FBHs have been recorded. You can see the experimental C-scans obtained on both series of FBHs on the following figure. Group #1 corresponds to FBHs located between 5 & 150 mm in depth while Group #2 corresponds to FBHs located between 10 & 60 mm in depth. The experimental echodynamic curves obtained are superimposed below. The maximum amplitude is obtained at a depth of 15mm.

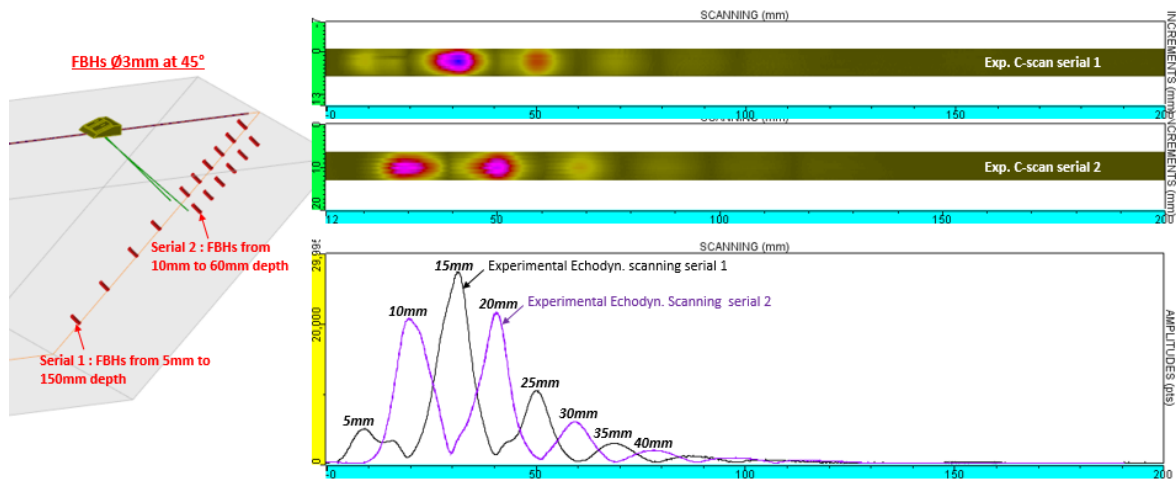


Figure 2. Experimental C-scans & echodynamic curves obtained for both groups of FBHs.

2.3 Comparison of simulation/experimental results

The « Depth - Amplitude » curves obtained experimentally and in the CIVA simulation are presented below for both models « KIR » and « KIR COMPLETE BEAM ». Both predictions give a fairly good agreement with the measurements, the discrepancy being generally lower than 2dB, except for the 10mm depth where it reaches 3dB. A slight improvement can be noticed of the agreement with the « KIR_COMPLETE » model for the larger depths and for the near field zone.

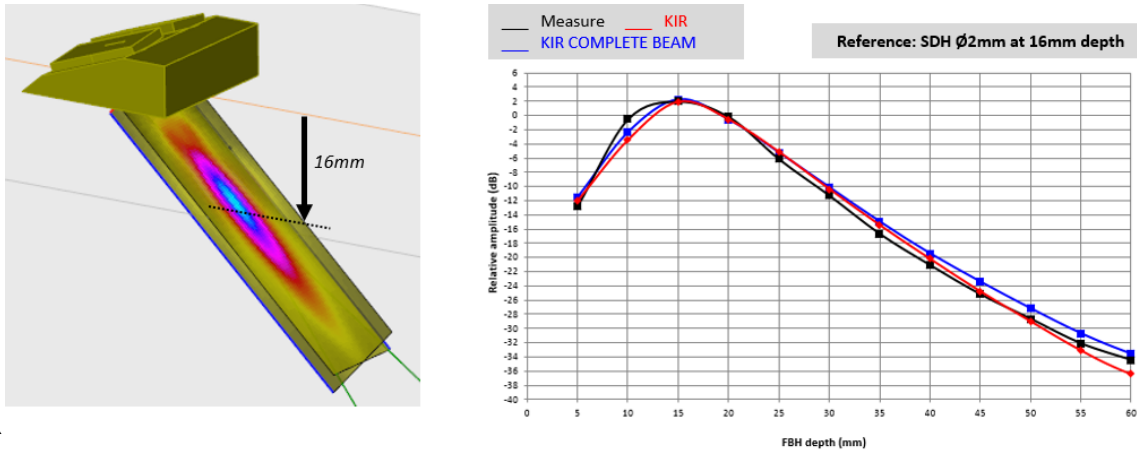


Figure 3. Image of the transmitted beam computation in a steel block. Comparison of « Depth-Amplitude » curves obtained by simulation (model « KIR » & « COMPLETE KIR ») and experimentally. Amplitude reference on a SDHØ2mm, 16 mm depth.

The superimposition of echodynamic curves and A-scans is presented on the following figure. It confirms the very good agreement between CIVA and the experiment, also on the signal shapes (versus time or versus scanning position). In addition to this, it is also possible to identify the part of the signal associated with the slight discrepancy seen at a depth of 10 mm. However, it's important to note that these discrepancies are in the same order of magnitude as the experimental uncertainty evaluated at +/-3 dB.

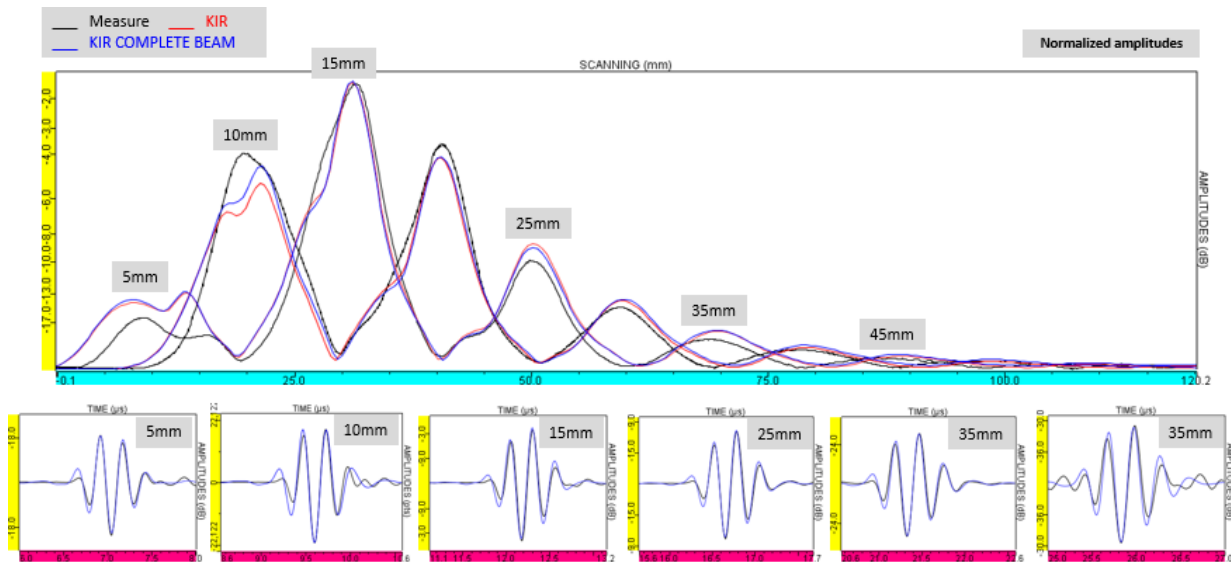


Figure 4. Comparison of echodynamic curves (along the scanning axis) and the A-scan signals obtained on the different FBHs (experiments in black, KIR and KIR COMPLETE models respectively in red and blue). Normalized amplitudes.

3. Tandem configuration

Tandem is an inspection technique commonly used for weld inspections, especially with the zonal discrimination approach [6].

3.1 Description of the configuration

The tested tandem configuration involves a linear phased-array (PA) probe of 64 elements, working at 5 MHz and mounted on a S45° Plexiglas wedge. The linear array parameters have been obtained from the manufacturer while the properties of the wedge have been measured (geometry, velocity, angle).

To create the tandem configuration with the PA probe, a group of elements is enabled to transmit the beam while other elements are active in reception. In this case, the transmission pattern is performed with 20 active & fixed elements while the reception mode is created with 10 elements working in electronic scanning. This reception mode generates a dynamic change of the shear waves crossing points in transmission and reception, from 32.5 mm to 50 mm in depth. The 7 sequences (seq) created are illustrated on the sketch below.

A delay law is applied to the transmission group creating a focusing along the beam axis (at 45 mm depth with a 45° angle). No delay laws are applied in reception. These focal laws have been imported from the acquisition files (note that CIVA can also compute focal laws).

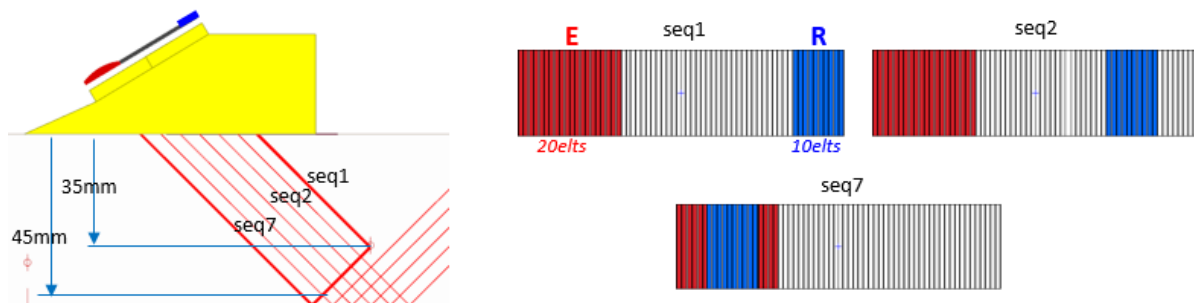


Figure 5. Tandem Configuration with a PA probe mounted on a S45° wedge.

The following figure shows an example of the radiated beam in Transmission/Reception for sequences 1 & 5, corresponding to shear wave axis crossing points around 32.5 mm & 44 mm in depth. The beam spot obtained has a size (along the vertical axis) of 9.5mm for sequence #1 and 10.8 mm for sequence #5, at -6dB.

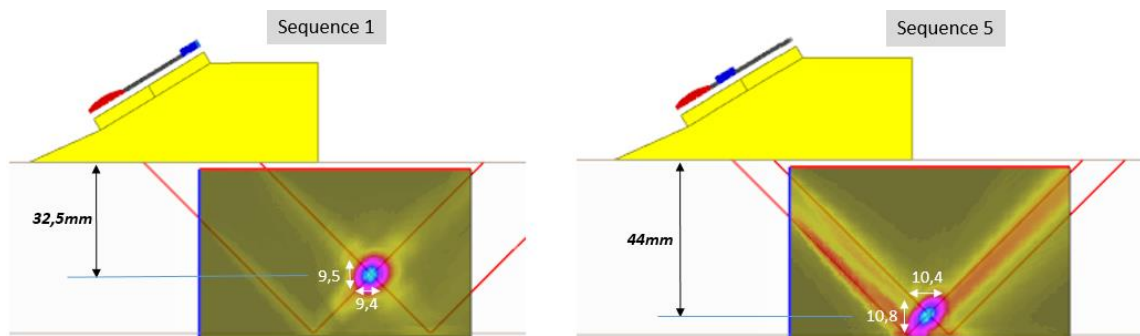


Figure 6. Ultrasonic field in the ferritic steel block. PA probe 64 elements 5MHz, sequences #1 & #5, shear wave at 45°, tandem mode.

A specific mock-up of 50 mm wall thickness in ferritic steel has been made in order to have available some embedded planar defects, necessary to predict the performance of CIVA in such a tandem configuration. It is made of 5 EDM notches of 5mm height initiated from the side of the specimen. For calibration, FBHs placed at different depths from the end of the

block have been machined so that they are oriented horizontally. Notches and FBHs are at the same depths (depths referenced at the center of the notches and the axis of the FBHs).

Defects are located each 5 mm in depth. Then, the defects' depths change from 27.5 to 47.5mm (or from 20mm to 5mm if you consider their ligament, that is to say the distance between the defect bottom and the back wall).

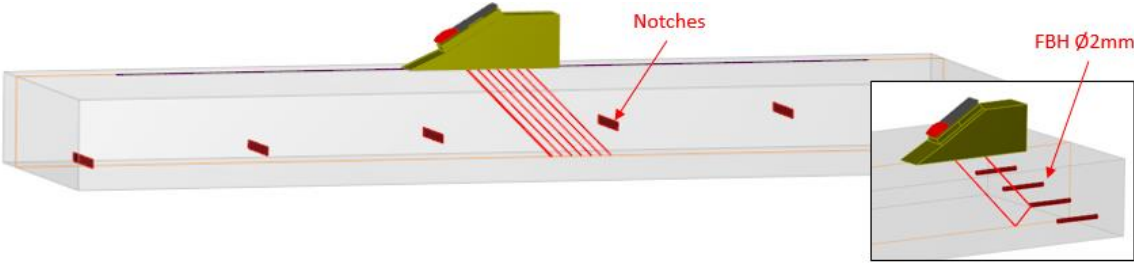


Figure 7. Mock-up used to evaluate CIVA performance for tandem configuration.

3.2 Acquisitions performed

C-scan acquisitions have been performed and the indirect signals obtained have been recorded, corresponding to the « TrbTdT » sound paths (« T » corresponds to T wave path, « rb » to the back wall reflection and « d » to the defect interaction). An example of experimental B-scans obtained for sequences 1 to 7 is shown in Figure 8. The whole set of curves showing the obtained amplitudes versus the ligament of the notches is then presented for all the relevant sequences where a signal amplitude can be measured (sequences 1 to 6). Amplitudes are normalized in comparison to the signal amplitude obtained with the FBH at a depth of 32.5 mm and detected with sequence #1. This variation shows the ability of the tandem mode to detect embedded defects with a similar sensitivity for various thicknesses and depth ranges.

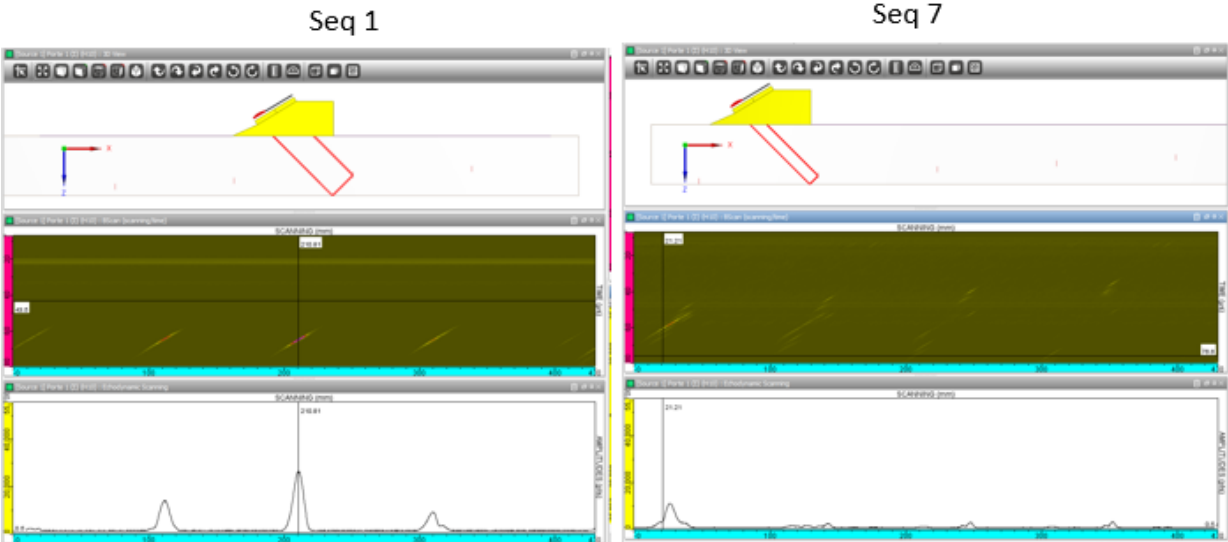


Figure 8. Experimental results obtained on notches. PA probes 5MHz, S45°, sequence #1 and #7, tandem mode.

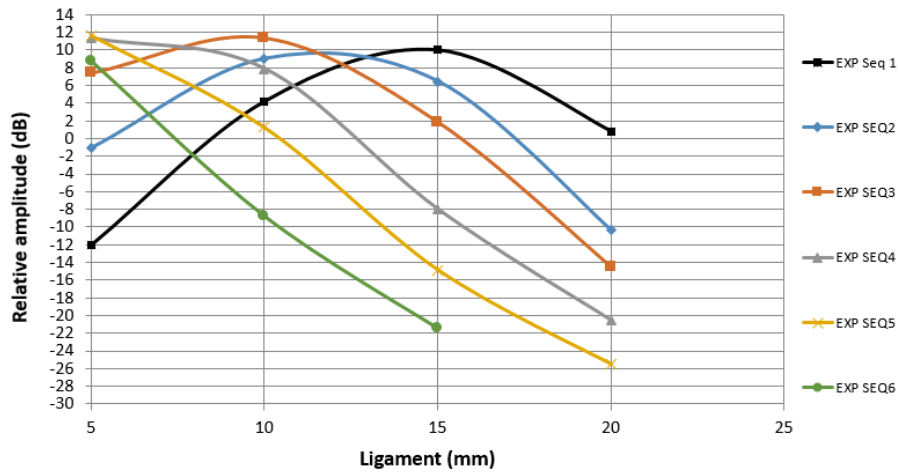


Figure 9. Amplitude/Ligament curves for notches and for sequences #1 to #6. Amplitude reference taken on a FBH Ø3mm at 32.5 mm depth (i.e. 15 mm ligament) detected with sequence #1. PA probes 5MHz, S45°, tandem mode.

3.3 Comparison of simulation/experimental results

The Amplitude/Ligament curves obtained by the simulation (KIR model) and experimentally are superimposed and shown on the following Figure 10, for a few of the electronic sequences (number #1, #3, #4 and #5). Regardless of notch depth, CIVA predicts signal amplitudes with a very good accuracy. A slight overestimation is observed for the sequence #1, but is only about 2dB, less than the measurement uncertainty estimated at 3dB. For most of the other cases, the amplitude differences are lower than 2 dB.

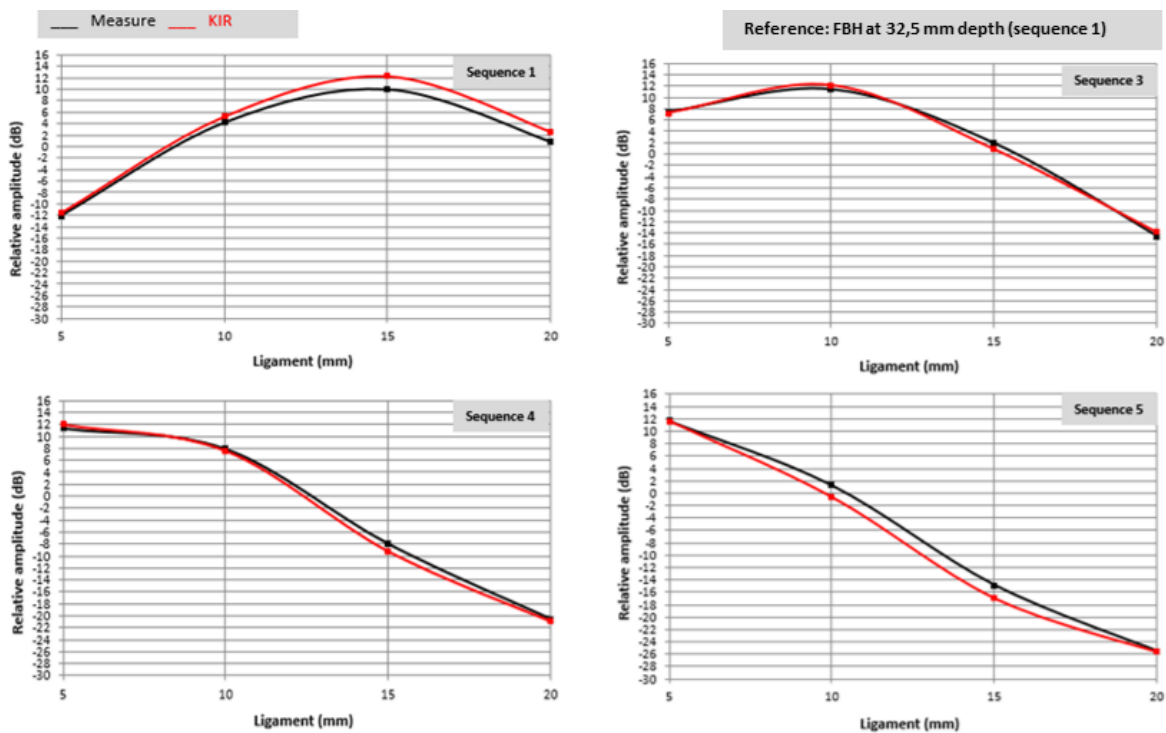


Figure 10. Comparison of Amplitude/Ligament (~depth) curves obtained with the simulation model (KIR) and experimentally on the notches. PA probe, 5MHz, S45°, Tandem mode.

The superimposition of echodynamic curves obtained on these notches is presented for a few sequences on the following Figure 11. Again it confirms a very good agreement between CIVA and the experiment on the signal shapes. Amplitudes are normalized with reference to the maximum amplitude obtained on each sequence.

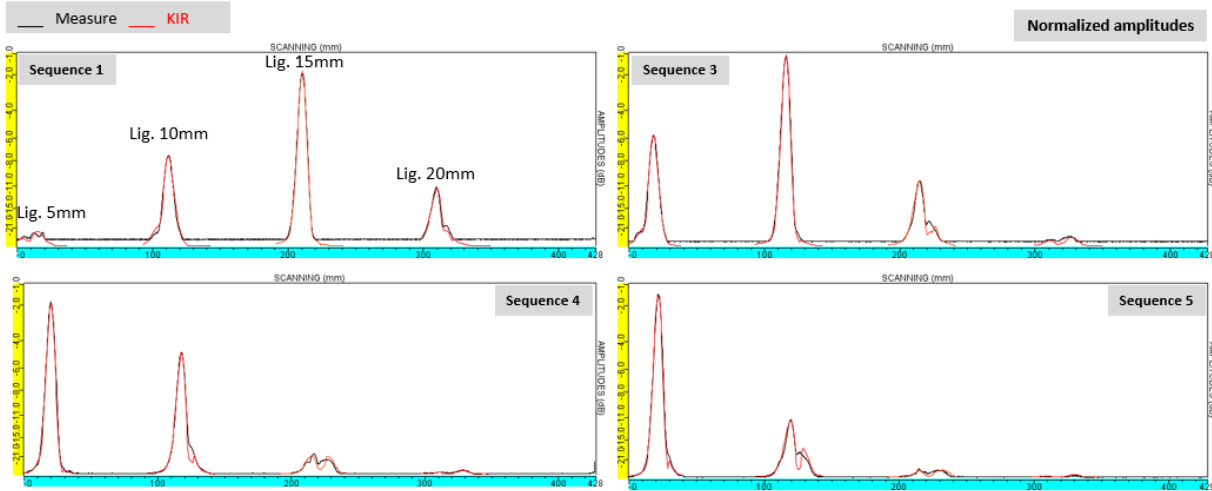


Figure 11. Comparison of echodynamic curves (along the scanning axis) obtained on the different notches (experiments in black, KIR model in red). Normalized amplitudes. PA probe, 5MHz, S45°, Tandem mode.

4. Conclusion

This paper presents comparisons between experimental acquisitions and simulations for different configurations using separate Transmission/Reception modes in the CIVA software.

In the first part, a dual element transducer is used. It is often very challenging to validate this type of probe due to the input parameters which are often difficult to know with sufficient accuracy (roof or incidence angles for instance). It is sometimes necessary to use radiography or to use reverse engineering methodologies to get the relevant information. The obtained simulation results are in a good agreement with the experimental results in regards to both the signal amplitudes and signal shapes versus time or scanning position, considering the experimental uncertainty (3dB).

In the second part, a tandem mode has been used to study echoes obtained on various notches embedded in a planar block and located at different depths. This configuration involves a 64 elements contact probe generating shear waves at 45°. An electronic scanning technique is applied to transmission and reception elements to cover various ranges of depths in the block. More precisely, 7 sequences are enabled successively to change the crossing point depth of shear waves from 32.5mm to 50mm in depth. The agreement with the experimental data is very good in terms of amplitudes (differences lower than 2dB) but also in terms of echo shapes for the different sequences considered.

You will find more information on these test cases as well as many other validation cases on the EXTENDE website [4].

References

- [1] CIVA website <http://www-civa.cea.fr>
- [2] Darmon, M, Chatillon, S, “Main Features of a Complete Ultrasonic Measurement Model: Formal Aspects of Modeling of Both Transducers Radiation and Ultrasonic Flaws Responses.” Open Journal of Acoustics, 3A (2013)
- [3] Calmon P, Recommendations for the use and validation of NDT simulation, V, IIW Best practice document, IIW 2363-13(2013).
- [4] EXTENDE website <http://www.extende.com>
- [5] <http://www.extende.com/reverse-engineering-for-dual-element-probes>
- [6] Chapuis, B., F. Jenson, P. Calmon, G. DiCrisci, J. Hamilton, and L. Pomié, “Simulation Supported POD Curves for Automated Ultrasonic Testing of Pipeline Girth Welds,” Welding in the World, Vol. 58, No. 4, 2014, pp. 433–441.